The Response of Surface Gravity Waves to Changing Wind Direction

H. GÜNTHER AND W. ROSENTHAL

Institut für Geophysik and Max-Planck-Institut für Meteorologie, Hamburg, Germany

M. DUNCKEL

Max-Planck-Institut für Meteorologie, Hamburg, Germany

(Manuscript received 15 July 1980, in final form 29 January 1981)

ABSTRACT

The behavior of a wind-sea is investigated for wave directions differing from the local wind direction. To describe the phenomenon we added the mean wave direction as an additional prognostic quantity to the JONSWAP parameters used in mathematical models of the wind-sea in previous publications (Hasselmann *et al.*, 1976; Günther *et al.*, 1979a,b).

A boundary is given for the frequency domain in which the spectral energy responds to a veering wind field.

1. Introduction

The description of surface gravity wave generation has developed rapidly during the last two decades. This includes the physical processes of momentum transfer from the atmosphere to the waves and the attenuation of wave motion (Garret and Smith, 1976; Snyder *et al.*, 1980; Hasselmann, 1974; Phillips, 1977; Miles, 1957, 1959) as well as the knowledge about the dynamics of energy flux in phase space of surface waves (Hasselmann *et al.*, 1973). The basic behavior of the energy distribution in a growing wind-sea for homogeneous stationary wind fields will be reviewed in Section 2. The basic equations for that case were first described by Mitsuyasu (1968)[1]. The constraint of a stationary and homogeneous wind strength is easily removed and numerical models yield reasonably good results as long as wind direction behaves quasi-stationary. That means as long as the wind direction can be considered constant for time differences within which the mean direction of the wave spectrum could turn into the wind direction.

A few comparisons of different wave models with sea truth for rapidly changing wind directions, especially in hurricanes, do exist (Cardone *et al.*, 1977). The power spectra compare reasonably well. Sea truth of the spatial distributions of mean wave directions in hurricanes was obtained only recently (King and Shemdin, 1978) and therefore has not yet been compared to the models.

The so-called NORSWAM model (Günther *et al.*, 1979a) provides good results in comparisons between modeled and observed one-dimensional energy spectra for wind direction changes occurring on time and space scales of midlatitude cyclones. However, Günther *et al.* (1979b) discovered systematic deviations between sea truth and model results for small-scale veering wind fields sampled during the JONSWAP 73 experiment. The deviations seemed to be caused by the crude directional assumptions included in the hybrid model. This motivated us to conduct a more systematic investigation of the response of wind waves to temporal changes of wind direction. We will devote this paper to the mathematical description of the effect and the experimental data supporting it; and in a later publication we will display the performance of the hybrid model, which includes directional parametrization of the wind-sea applied to complex field situations.

The field data from JONSWAP 73 shown here already have been discussed in D. E. Hasselmann *et al.* (1980). These authors describe the directional relaxation of individual frequency bands by means of a relaxation time. The behavior of the direction for individual frequency bands is not suitable for our ultimate purpose of simulating the surface wave field by a model, nor is it suitable for rather mixed swell wind-sea situations in which a clear spectral separation of both of these parts has not already taken place. We feel that the valid description of the spectral directional fine structure under the combined action of nonlinear wave-wave interaction and wind changes on a rather small scale in

[1] Mitsuyasu, H., 1968: On the growth of the spectrum of wind-generated waves. I. *Res. Inst. Appl. Mech., Kyushu Univ.*, Rep. No. 55, 459–482.

0022-3670/81/050718-11$06.75

space and time is beyond our present abilities. We discuss possible steps to improvement at the end of Section 3. Therefore, our considerations, presented below, result in a definition of a relaxation time averaged over all frequencies, which react to a differing wind direction. In addition, we propose a border for the frequency region, for which the averaged wave direction turns into wind direction.

Nonlinear interaction in wind-driven surface waves has been shown to be the main shape-stabilizing mechanism for the energy spectrum (Hasselmann *et al.*, 1973; 1976) and has been successfully included in most recent wind-sea models (Toba, 1978; Resio and Vincent, 1979; Günther *et al.*, 1979a,b).

As a result, momentum transferred from the atmosphere to the surface waves is distributed over all frequencies by the nonlinear interaction mechanism. This mechanism, therefore, should also be taken into account for momentum input direction, which deviates from the mean wave direction.

We therefore use the mathematical formalism of Hasselmann *et al.* (1976) to include differing directions of the wind and the averaged wave field in a parametric wind-sea model. In models of this kind, the wind-sea is treated as a statistical ensemble of interacting wave modes which is best described by ensemble properties (using appropriate parameters) rather than properties of the single wave modes.

In Section 2 we review the known development of a wind sea for homogeneous stationary wind fields and present the basic ideas of our mathematical model of surface waves.

In Sections 3 and 4 we describe the derivation of the prognostic equation for the directional parameter, and in Section 6 the relaxation time in that equation is deduced from measurements. In Section 5 the modification of the low-frequency limit of the wind-sea is discussed.

2. The behavior of a developing wind-sea and the definition of swell

As an example of the behavior of a developing wind-sea, we review the stationary ideal fetch limited deep water case for an offshore wind blowing perpendicular to a long straight coastline. In this case the different wave modes, characterized by their frequency f and propagation direction δ, are described as a statistical ensemble of interacting "particles". The mean shape of the spectrum is shown in Fig. 1. The following ensemble parameters are chosen for describing the wind sea:

- The peak frequency f_m.
- The Phillips parameter α that describes the f^{-5} decrease of the high-frequency tail of the spectrum

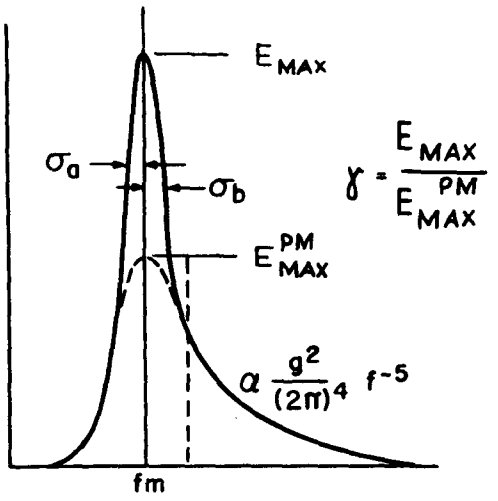

FIG. 1. The definition of the JONSWAP parameters for a wind-sea spectrum.

- The peak enhancement factor $\gamma = E_{peak}/E_{PM}(f_m)$ between the peak energy E_{peak} and the peak $E_{PM}(f_m)$ of the Pierson-Moskowitz-type spectrum $E_{PM}(f)$ with the same f_m and α: (1)

$$E_{PM}(f) = \frac{g^2 \alpha f^{-5}}{(2\pi)^4} \exp\left[\frac{-5}{4}\left(\frac{f}{f_m}\right)^{-4}\right], \quad (2)$$

- The left-hand peak width $\sigma = \sigma_a$ for $f \leq f_m$.
- The right-hand peak width $\sigma = \sigma_b$ for $f > f_m$.

The one-dimensional model spectrum is written

$$E(f) = E_{PM}(f) \exp\{\ln\gamma \cdot \exp[-(f - f_m)^2/2\sigma^2 f_m^2]\}. \quad (3)$$

Fig. 1 gives the meaning of the five parameters. For a more detailed description of the numerical connection between a specific spectrum and its connected parameters we refer to Müller (1976).

The directional distribution of the full two-dimensional spectrum can be written with a directional distribution function $R_f(\delta)$

$$F(f, \delta) = E(f) R_f(\delta), \quad (4)$$

so that

$$E(f) = \int d\delta F(f, \delta). \quad (5)$$

The exact shape of the directional distribution apart from the mean direction does not seem to be critical for our purposes. We use

$$R_f(\theta) = R_f(\theta, \theta_0) = \begin{cases} 2\pi^{-1} \cos^2(\theta - \theta_0), & \text{for } |\theta - \theta_0| \leq \pi/2 \\ 0, & \text{for } |\theta - \theta_0| \geq \pi/2. \end{cases} \quad (6)$$

Here θ_0 is the mean direction of the wind-sea. For

stationary, homogeneous cases, θ_0 is the direction of the wind vector.

With increasing fetch the peak frequency approaches the Pierson-Moskowitz frequency

$$f_{PM} = 0.13 \times \frac{g}{U_{10}}, \quad (7)$$

where g is the gravitational acceleration (9.81 m s^{-2}) and U_{10} the local wind strength at a height of 10 m above the sea surface. The Phillips parameter α decreases to the limiting value 0.0081 and the peak enhancement factor γ drops from its mean value 3.3 toward 1.

The establishment of the self-similar shape shown in Fig. 1 of the wind-sea spectrum has been successfully simulated by numerical calculation of the Boltzmann integrals for the interacting wave modes (see figs. 2.16–2.21 in Hasselmann *et al.*, 1973). Also, the migration of the spectral peak toward lower frequencies has been demonstrated by computer experiments (Hasselmann *et al.*, 1973) to be due to nonlinear interaction. However, at present there is only a qualitative understanding of the existence of the lower limit for that migration, e.g., the Pierson-Moskowitz frequency. Although this may be overcome in future through the application of more powerful integration software, in this publication we will treat the concept of the limiting Pierson-Moskowitz frequency as an experimentally proven fact. Experimental material for the transition to the fully developed state with $f_m = f_{PM}$ is given by Ewing (1980). The necessary extension of this concept to the case of veering winds is one subject treated in Section 5 and will allow us to demonstrate that low frequency surface waves do not respond to turning winds.

The energy and momentum of those surface wave modes, which are in a frequency domain greater than the local Pierson-Moskowitz frequency, will be referred to as "wind-sea" in this paper as long as the connected mean wave direction is parallel to the local wind vector. Energy propagating in wind direction in frequency bands less than f_{PM} is denoted as "swell".

This frequency border f_{PM} is of course not a sharp one in nature. For instance, the limiting case of a wind-sea spectrum is the Pierson-Moskowitz-type (2) which has the energy density peak at frequency $f_m = f_{PM}$ and there also is energy in frequency bands slightly less than f_{PM}, diminishing rapidly with decreasing frequency.

Surface waves belonging to the swell domain are not influenced by the local wind. The swell energy of a special propagation angle and frequency band is advected by its associated group velocity.

3. The inclusion of direction into the wind-sea parametrization

The concept of wind-sea parametrization and the translation of the spectral energy balance equation

$$\frac{F(\mathbf{r}, f, \delta)}{\delta t} + \mathbf{v}(f, \delta)\cdot\nabla F(\mathbf{r}, f, \delta) = T(\mathbf{r}, f, \delta), \quad (8)$$

[where $\mathbf{r}$ is the location, δ the propagation direction (rad), f frequency (Hz), $\mathbf{v}$ the group velocity, F the two-dimensional energy density spectrum and T the appropriate source function] into prognostic equations for the parameters has been treated in previous publications (Hasselmann *et al.*, 1976; Günther *et al.*, 1979a). Tests have been carried out successfully, which indicate that our concept of parametric wind-sea description together with a swell propagation treatment originally introduced by Barnett *et al.* (1969)[2] is able to simulate surface waves for many wind situations. We think it is advantageous to give a summary of the simulation of the surface wave field in our hybrid model because the scheme is set up to reveal the natural processes closely. According to the classification of the surface wave field in wind-sea and swell, we use a hybrid model in which the wind-sea is described by the ensemble parameters, which obey the associated prognostic equations. The wave energy not included in this parametric description is treated in a discrete spectral-type part of our hybrid model by using characteristics similar to Barnett *et al.* (1969).

Special care must be taken if energy must be exchanged between the two parts of the hybrid model, which is necessary:

1) If the wind drops to a point where the associated Pierson-Moskowitz frequency lies above the local peak frequency f_m. (Wind-sea energy transferred to characteristics.)

2) If the peak frequency f_m has become less than frequency bins of the characteristic part of the model with non-vanishing energy. (Energy picked up by the wind sea.)

This exchange is described in detail in Günther *et al.* (1979a). In the first case, the procedure is to describe the new spectrum by a fully developed sea with $f_m = f_{PM}$ characterized by the new wind velocity, and shift the difference energy between old and new wind-sea at each frequency band to the characteristics. Energy in characteristic frequency

[2] Barnett, T. P., C. H. Holland, Jr., and P. Yager, 1969: A general technique for wind-wave prediction, with application to the South China Sea. Contract N 62 306-68-C-0285, U.S. Naval Oceanogr. Office, Washington, DC.

bins higher than the local f_m is then reabsorbed in the wind-sea by increasing the α parameter.

In the second case, the energy is purged on the characteristics with frequency $> f_m$, and the wind-sea energy is increased by the same amount. The physical interpretation, in the first case, is that after a wind drop the energy present in the wind-sea domain will relax to the Pierson-Moskowitz spectrum connected with the new wind velocity, while the energy in the swell region will leave the area by means of simple advection without sources or sinks.

The interpretation in the second case is that the energy is redistributed in the wind-sea domain by a nonlinear interaction to achieve the self-stabilized shape.

The parameters chosen in Section 2 for the one-dimensional wind-sea energy spectrum show very different temporal behavior. Calculations of nonlinear spectral shape restoring processes show that γ, σ_a, and σ_b relax to equilibrium values on a much faster time scale than f_m and α. The relaxation time of the wind-sea to the prevailing wind direction is of the same order of magnitude as that for γ, σ_a, and σ_b, as can be seen from the field measurements discussed in Section 6. In previous applications of the hybrid wave model this rather rapid relaxation justified our approximation of the turning of the wind-sea into wind direction by an instantaneous process, keeping the mean wave direction always aligned with the wind direction. This approximation gives reasonable results for moderately rapid wind direction changes. Errors are observed, for instance, during frontal passages with essentially instantaneous changes in wind direction.

To get an impression of what happens after a change of the wind direction, we look at Fig. 7a which is one of our field data sets which we will discuss in more detail in section 6. We notice that the one-dimensional energy spectrum does not change remarkably. However, looking at the mean direction $\delta_0(f)$ of the different wave frequencies (Fig. 7b) it can be seen that the short waves adapt to the new wind direction rapidly while the low frequencies appear to take up the new momentum direction from the higher frequencies with some delay. Due to the transfer of energy and momentum from high to low frequencies by nonlinear interaction, it seems obvious that after a change in wind direction momentum in the new direction is given to the high-frequency tail of the spectrum first and then this momentum direction propagates by nonlinear interactions to lower frequencies until the whole spectrum has a mean direction parallel to the new wind direction.

As a first parameter to describe this directional behavior, we choose the mean direction averaged over the wind-sea spectrum. The wave momentum $\mathbf{m}(f, \delta)$ for a frequency-direction band (f, δ) is described by the energy $F(f, \delta)$ and the phase velocity $c(f)$

$$\mathbf{m}(f, \delta) = \frac{F(f, \delta)}{c(f)} \mathbf{n}(\delta), \tag{9}$$

where $\mathbf{n}(\delta)$ is a unit vector pointing into the wave direction δ, and δ is counted clockwise from north. The components in the x (east) and y (north) directions are

$$\left.\begin{aligned} m_x(f, \delta) &= |\mathbf{m}(f, \delta)| \sin\delta \\ m_y(f, \delta) &= |\mathbf{m}(f, \delta)| \cos\delta \end{aligned}\right\}. \tag{10}$$

We define the total momentum along the coordinate axis by

$$\left.\begin{aligned} M_x &= \int df d\delta m_x(f, \delta) \\ M_y &= \int df d\delta m_y(f, \delta) \end{aligned}\right\}. \tag{11}$$

The mean direction θ_0 of the spectrum is defined as the direction of the vector

$$\mathbf{M} = (M_x, M_y), \tag{12}$$

which is given by

$$\left.\begin{aligned} \sin\theta_0 = M_x/|\mathbf{M}|, \quad \cos\theta_0 = M_y/|\mathbf{M}| \\ \theta_0 = \arctan M_x/M_y. \end{aligned}\right\}. \tag{13}$$

Since θ_0 is a quantity derived by integrating over frequency, it can provide us with information on the directional distribution over frequencies only in special situations. For simple cases we can qualitatively deduce the mean direction $\delta_0(f)$ in frequency space, since we know that the high frequencies adapt to the new wind direction very rapidly and the main spectral energy, which determines the θ_0 value, is centered around the peak frequency f_m. In more complicated cases, for instance intermittent clockwise and anticlockwise wind shifts (as shown in Fig. 2), $\delta_0(f)$ cannot be reproduced from a knowledge of θ_0. To describe these cases we have to introduce further directional parameters. We decided, however, that the experimental evidence is not sufficient to determine the relaxation of the directional parameters in addition to θ_0. That means we have chosen the spectral functions defined by (3), (4) and (6) for an approximate description of the wind-sea spectra with θ_0 defined by (13).

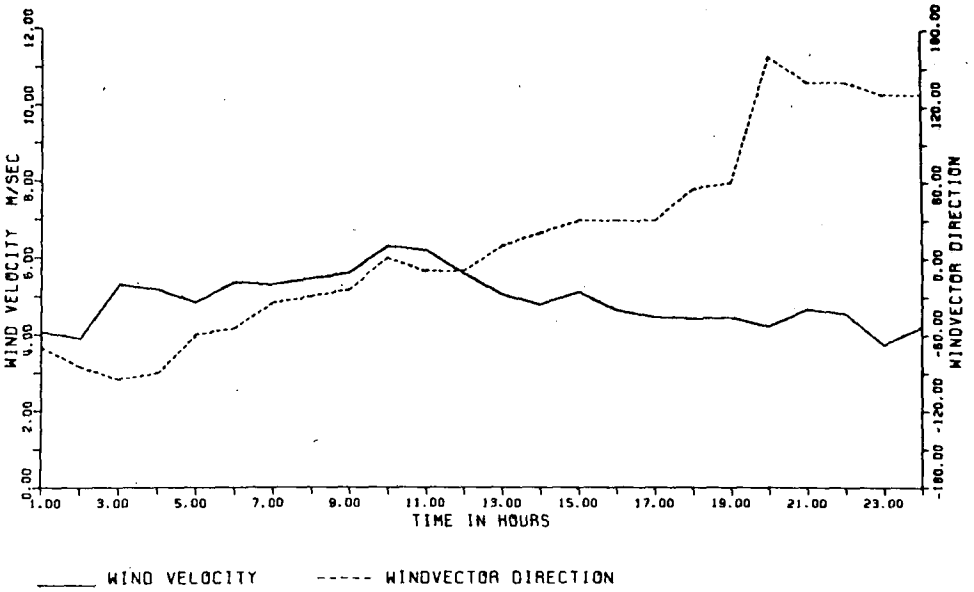

FIG. 2. Wind history on 13 September 1973 derived from hourly measurements at a tower near the meteorologic buoy.

4. The parametrical equations including the mean direction θ_0

Since we are now including direction in the description of the wind-sea, the master equation is written for each wave component in wavenumber space in terms of the momentum $\mathbf{m}(f, \delta)$ instead of energy $F(f, \delta)$ as done in (8). The ratio of $F(f, \delta)$ and $|\mathbf{m}(f, \delta)|$ is the phase velocity $c(f)$ [Eq. (9)]. The transport equation for each wave component is

$$\left.\begin{aligned} &\frac{\partial \mathbf{m}(f, \delta)}{\partial t} + [\mathbf{v}(f, \delta)\cdot\nabla]\mathbf{m}(f, \delta) = \tau \\ &\tau = \tau_{\text{in}}(f, \delta) + \tau_{\text{nl}}(f, \delta) + \tau_{\text{dis}}(f, \delta) \end{aligned}\right\} . \quad (14)$$

τ is the source function for the spectral momentum density, and as usual divided into atmospheric input τ_{in}, dissipation τ_{dis} and nonlinear contribution τ_{nl}.

We construct our functionals operating on $\mathbf{m}(f, \delta)$ such that we reveal the parameters of the one-dimensional spectrum. Since

$$E(f) = c(f) \int d\delta [m_x^2(f, \delta) + m_y^2(f, \delta)]^{1/2}, \quad (15)$$

we can use the functionals $\Phi_i[E(f)], i = 1, \ldots, 5$, defined in Günther *et al.* (1979a), to arrive at the JONSWAP parameters defining the shape of the one-dimensional spectrum:

$$\left.\begin{aligned} a_i = \Phi_i(\mathbf{m}) = \Phi_i\Big\{c(f) \int d\theta [m_x^2(f, \theta) + m_y^2(f, \theta)]^{1/2}\Big\} \\ f_m = a_1, \quad \alpha = a_2, \quad \gamma = a_3, \\ \sigma_a = a_4, \quad \sigma_b = a_5 \end{aligned}\right\} . \quad (16)$$

The parameter $\theta_0 = a_6$ is already given by (13).

When mapping Eq. (14) into the parameter space we arrive at

$$\left.\begin{aligned} &\frac{\delta a_i}{\delta t} + D_{ijx}\frac{\delta a_j}{\delta x} + D_{ijy}\frac{\delta a_j}{\delta y} = S_i, \\ &\qquad i, j = 1, \ldots, 6 \\ &D_{ijx} = \Phi_i'\left(v_x \frac{\delta \mathbf{m}}{\delta a_j}\right) \quad D_{ijy} = \Phi_i'\left(v_y \frac{\delta \mathbf{m}}{\delta a_j}\right) \\ &S_i = \Phi_i(\tau) \qquad\qquad v_x = |\mathbf{v}| \sin\delta \\ &\qquad\qquad\qquad\quad v_y = |\mathbf{v}| \cos\delta \end{aligned}\right\} . \quad (17)$$

Here $\Phi_i', i = 1, \ldots, 6$, are the functional derivatives of the Φ_i in (16) and (13), respectively. Φ_6' is shown in the Appendix. Details of $\Phi_i, i = 1, \ldots, 5$, are given in Hasselmann *et al.* (1973) and Günther *et al.* (1979a). The calculation of the D_{ijx}, D_{ijy} and S_i also is given in the Appendix if $i = 6$ and/or $j = 6$.

5. The definition of the swell region after a change in wind direction

As has been described in section 2 the Pierson-Moskowitz frequency (7) is the heuristic lower limit for the peak frequency f_m of a wind-sea spectrum aligned with the local wind direction. The total source function $S_i, i = 1, \ldots, 5$, therefore vanishes at this stage (if the other parameters are also at their equilibrium value). We can compare this with the behavior of the source function from the spectral description section 3, which we approximate by the source function proposed by Snyder and Cox (1966):

$$T_U(\mathbf{r}, f, \theta) \approx [\mathbf{k}(f, \theta)\cdot\mathbf{U}(\mathbf{r}) - 2\pi f]F(f, \theta) \qquad (18)$$

$$= 0 \quad \text{if} \quad [\mathbf{k}(f, \theta)\cdot\mathbf{U}(\mathbf{r}) - 2\pi f] \leq 0.$$

Snyder and Cox estimated the height in which $\mathbf{U}(\mathbf{r})$ is measured to be equal to the wavelength $\lambda = 2\pi/|\mathbf{k}|$. This is a parameter which depends on local atmospheric conditions and air-sea temperature difference and is not easily accessible. We may therefore estimate $U(\mathbf{r})$ to be introduced in (18) from the consideration that, if $\mathbf{U}$ in (18) is replaced by $1.22\ U_{10}$, this equation becomes consistent with (7), giving the lower limit of non-vanishing source function. That means the solution of

$$T_U(\mathbf{r}, f, \theta_w) = 0, \qquad (19)$$

where θ_w is the direction of wind vector and $\mathbf{U} = 1.22\cdot\mathbf{U}_{10}$, is given by (7). For this reason, instead of giving the height, where $U(r)$ is to be measured we use $1.22\cdot U_{10}$ as an estimate for $U(r)$.

From (19) we conclude that the frequency border f_b between swell and wind-sea domain should be defined angle dependent by

$$T_U(r, f_b, \delta) = 0, \quad U = 1.22U_{10}, \qquad (20)$$

or explicitly

$$f_b = f_b(U_{10}, \theta_w, \delta)$$

$$= \begin{cases} 0.13\dfrac{g}{U_{10}\cos(\delta - \theta_w)}, & \text{for} \quad |\delta - \theta_w| < \pi/2 \\ \infty, & \text{elsewhere.} \end{cases}$$

That means, only energy in frequency and direction bands larger than $f_b(U_{10}, \theta_w, \delta)$ constitutes the wind-sea. In case of a wind and wave direction difference of $\pm\pi/2$ or more, for instance, the whole frequency range belongs to the swell region. This concept of vanishing source function for waves and wind direction, differing by nearly or more than 90°, has been used already by Donelan (1977)[3] and Kawai *et al.* (1979). We will find further confirmation for the concept, that only the frequency domain above f_b has non-vanishing momentum input into the surface wave field, in the field cases inspected in the next section. As in the beginning of Section 3, a description will be given of the implications of the new swell/wind-sea border for the wave energy exchange between the two parts of our hybrid model.

In the beginning of Section 3 we described the procedures of energy exchange between the wind-sea part and the swell part of our hybrid model. The frequency border between both parts was the Pierson-Moskowitz frequency from (7). This concept was sufficient for parallel wind direction θ_w and windsea direction θ_0. We extend it now for $\theta_0 \neq \theta_w$ and use $f_b[U_{10}, \theta_w(\text{new}), \theta_0]$ instead of f_m in the model description of energy transfer from wind-sea to swell given in Section 3.

In case swell energy advances in areas where its frequency and direction belong to the wind-sea region, this energy will be distributed by nonlinear wave-wave scattering processes to become a JONSWAP-type self-similar spectrum. In our hybrid model, we will approximate this effect by purging the swell energy at frequencies higher than the local wind-sea peak and by an instantaneous change of the wind-sea parameter set so that the sum of energy and momentum of the swell beam and the old wind-sea is reproduced in the energy and momentum of the new wind-sea. For convenience, we define the nondimensional peak frequency

$$\nu'' = \frac{U''f_m}{g} = f_m\frac{U_{10}}{g}\cos(\theta_w - \theta_0), \qquad (21)$$

where θ_w is the wind direction and θ_0 is as defined in (13); ν'' for $\theta_w = \theta_0$, of course, becomes the well known non-dimensional peak frequency $\nu = U_{10}f_m/g$ usually used in the literature.

6. Determination of the source function for θ_0 from field data

The experimentally determined statistical dependence of α and ν already has been used to find the source function for the energy spectral parameters (Hasselmann *et al.*, 1976; Günther *et al.*, 1979a). In the same manner we use experimental data to find the missing constant in the source function for θ_0, defined in the Appendix. The prognostic equation for $\theta_0 = a_6$ is from (12).

$$\frac{\delta a_6}{\delta t} + \sum_{\substack{i=1,5 \\ j=1,2}} D_{6ij}\frac{\delta a_i}{\delta x_j} = S_6 = -\chi U_\perp\frac{f_m^2}{g}, \qquad (22)$$

where $U_\perp$ is the wind vector component perpendicular to wave direction θ_0. For spatially homogeneous cases this equation simplifies to

$$\frac{\delta a_6}{\delta t} = -\chi U_\perp\frac{f_m^2}{g} = -\chi\frac{f_m^2}{g}U\sin(\theta_w - \theta_0). \qquad (23)$$

To use (23) for determining χ from field data we must look for cases which can be considered to have spatially homogeneous $a_1, \ldots, a_6$, which means that the one-dimensional energy spectrum should not change in space. We need pairs of such measurements, sufficiently close in time to replace the time derivation in (23) by the ratio of the differences $\Delta a_6/\Delta t$. During the JONSWAP 73 experiment four events occurred which could be used for our purpose. However, all of them are characterized by low wind speed and a spectral peak much less than the Pierson-Moskowitz frequency. The one-dimensional spectrum does not show a partition in swell

[3] Donelan, M. A., 1977: A simple numerical model for wave and wind stress prediction. Canada Center for Inland waters (unpublished report).

TABLE 1. Summary of parameters from our four cases. All angles are in degrees. $\theta_0(t_1)$, $\theta_0(t_2)$ are mean wave directions counted clockwise from north. θ is the "effective angle" between wind and wave direction derived from (27).

Case	Station no.	Date	Wind speed ($m\ s^{-1}$)	Direction of wind vector (deg)	Lowest frequency f_m influenced by turning wind (Hertz)	θ (deg)	t_1 (LT)	$\theta_0(t_1)$	t_2 (LT)	$\theta_0(t_2)$	χ (deg)
a	8	13/9/1973	4.5	60	0.33	31	1800	32	1910	54	0.20
b	8	13/9/1973	4.5	changing 60–150	0.32	32	1910	54	2000	62	0.12
c	8	13/9/1973	4.5	140	0.43	49	2100	57	2200	85	0.12
d	10	21/9/1973	7.0	270	0.36	−59	0815	−51	1019	−86	0.06
											$\chi = 0.12$ deg $= 0.21 \times 10^{-2}$ rad

and wind sea. To get an estimate of χ, in spite of this, we have to use some assumptions:

- The spectral energy responding to the change of wind direction can be approximated by a JONSWAP-type spectrum with the peak frequency given by

$$f_m = f_b[U_{10}, \theta_w(\text{new}), \theta_0] = \frac{0.13 \times g}{U_{10} \cos(\theta_0 - \theta_w)} \quad |\theta_0 - \theta_w| < \frac{\pi}{2} \tag{24}$$

or the equivalent equation

$$\nu'' = 0.13 \quad \text{with} \quad |\theta_0 - \theta_w| < \frac{\pi}{2}$$

- The lowest frequency in the experimental data that responds to the change in wind direction is a good approximation for f_m.

The wind situation as measured at the central station in hourly intervals for the 13 September 1973 is shown in Fig. 2. The variations of wind speed during the wave measurements can be neglected, but the variation of wind direction, which is also influenced by sampling variability and errors of the wind measurements, gives only a rough estimate of the angle $\theta_w - \theta_0$ necessary for Eq. (23) to determine χ. We decided, therefore, to use (24) to calculate an effective angle $\theta = (\theta_w - \theta_0)_e$ and show that the wind direction calculated from θ to be

$$\theta_w = \theta + \theta_0 \tag{25}$$

lies within the measured wind angle range. The parameter f_m in (24) is determined from the field data according to our second assumption. That gives

$$\cos\theta = \frac{0.13g}{Uf_m}. \tag{26}$$

The lowest frequency, which turns into the new wind direction, can be determined quite accurately, as can be seen in Figs. 3, 4, 5 and 7. This frequency is regarded as the peak frequency f_m of our model wind-sea. Now (26) determines the effective angle θ, which is then used to derive χ from the difference approximation of (23), i.e.,

$$\frac{|\Delta a_6|}{\Delta t} = \frac{|a_6(t_2) - a_6(t_1)|}{t_2 - t_1} = \chi \frac{f_m^2}{g} U \left[1 - \left(\frac{0.13 \times g}{Uf_m}\right)^2\right]^{1/2}, \tag{27}$$

where t_1, t_2 are the times of two adjacent determinations of a_6. The data we use are gathered with the meteorological buoy (MB) of the Institute for Meteorology, University of Hamburg and with a Pitch-and-Roll buoy (PR) of IOS Wormley. As already mentioned, they are described in detail by D. E. Hasselmann *et al.* (1980). Ten minute wind averages from MB and the nearby central station 8 are available at hourly intervals.

We discuss the individual cases in the following paragraphs. A summary of the relevant data is given in Table 1. From our four cases we get an average value of

$$\chi = 0.12° = 0.21 \times 10^{-2} \text{ rad}. \tag{28}$$

The largest uncertainty comes from the determination of the angular difference between wind and waves, which is represented by the square root in (27). The value of f_m in that root can be determined by an accuracy of about ± 0.02 Hz which results in an error of $\pm 30\%$ for the χ value of (28). For small angles $\theta = \theta_w - \theta_0$, Eq. (23) can be written as relaxation type equation

$$\frac{\delta\theta}{\delta t} = -\frac{\theta}{\tau} \tag{29}$$

with

$$\tau = \left(\chi \frac{f_m^2}{g} U\right)^{-1}. \tag{30}$$

The solution

$$\theta = \theta(t = 0)e^{-t/\tau} \tag{31}$$

means that the wind-sea requires a time τ to become approximately aligned with the wind, if it differs in direction by an angle θ ($t = 0$) at the beginning. To give a numerical example we find from (29) $\tau = 6.48$ h for $U = 20$ m s^{-1} and $f_m = 0.1$ s^{-1}.

The result (28) or (30) can be compared with the parameters derived by Hasselmann *et al.* (1980). These authors investigated the directional relaxation of the mean propagation direction $\nu_0(f)$ for individual frequency bands by fitting the equation

$$\frac{\partial \nu_0(f)}{\partial t} = 2\pi f b \sin[\delta_w - \nu_0(f)] \tag{32}$$

to a data set partially overlapping with the one used in this paper. They found

$$b \approx 3 \times 10^{-5}. \tag{33}$$

The relaxation described by (32) for single frequencies is not equivalent to our description of temporal directional behavior averaged over the frequencies. But in cases where both descriptions are applicable the relaxation to the wind direction should be of comparable magnitude. Using our Eq. (23) we may compare $2\pi f b$ for $f = f_m$ with $\chi(f_m^2/g)U$. If we choose the Pierson-Moskowitz limit 0.13 for Uf_m/g, we get

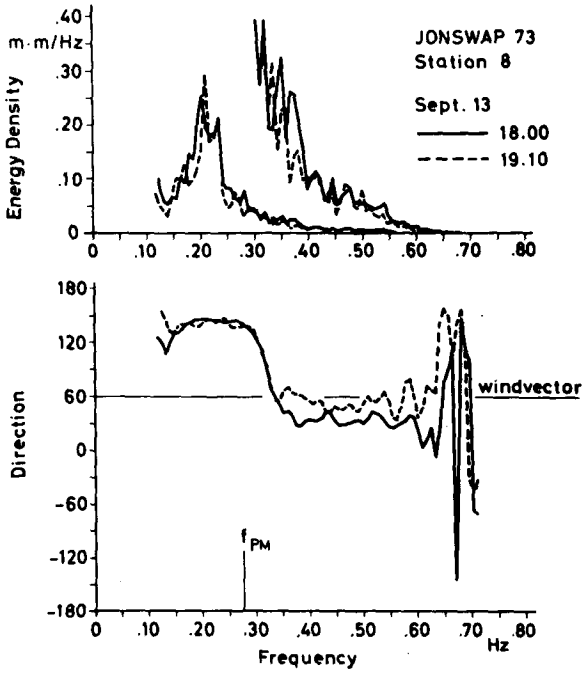

FIG. 3. (a) Power spectra for case a. The high-frequency region is shown 10 times enlarged. (b) The average wave direction spectra for case a. f_{PM} is the Pierson-Moskowitz frequency defined in (7).

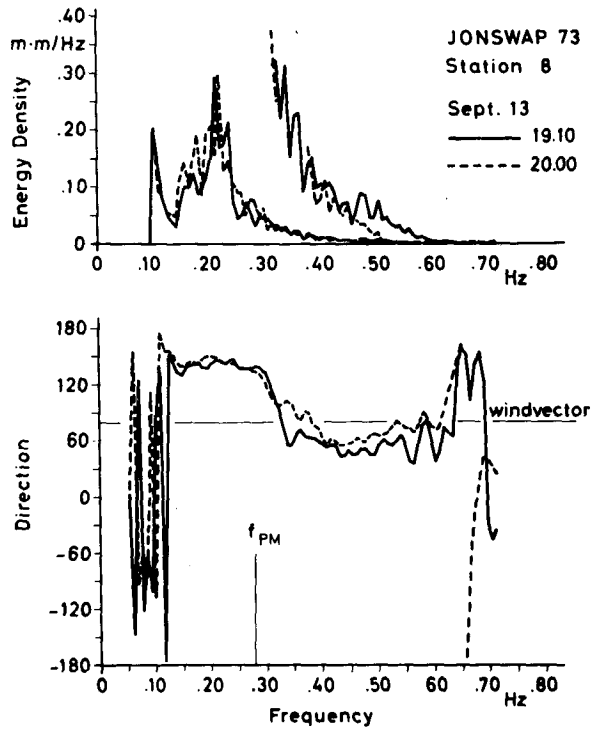

FIG. 4. (a) Power spectra for case b. The high-frequency region is shown 10 times enlarged. (b) The average wave direction spectra for case b. f_{PM} is defined in (7).

$$\chi f_m \times 0.13 = 0.27 \times 10^{-3} f_m \tag{34}$$

and, with (33),

$$2\pi f_m b = 0.19 \times 10^{-3} f_m.$$

Thus both results are of the same order of magnitude.

a. 13 September 1973 1800–1910 LT (MB) at station 8

The spectra of energy and mean direction are given in figs. 3a and 3b. The power spectra in Fig. 3a do not differ, allowing for the clearly visible scatter of the spectral energy density. The mean direction changes for frequencies higher than 0.33 Hz. The effective directional difference between wind and waves derived from (26) is $\theta = 31°$. This may be compared with the directional difference of 20° between wind and waves at 1800.

b. 13 September 1973 1910–2000 LT (MB) at station 8

The spectra are depicted in Figs. 4a and 4b. This case looks more complicated than case a because the energy bands influenced by the turning wind show no clear indication that at high frequencies energy is more aligned with the wind. Apparently, we see in the directional spectrum the wind history during the past 50 min, which is not resolved in our

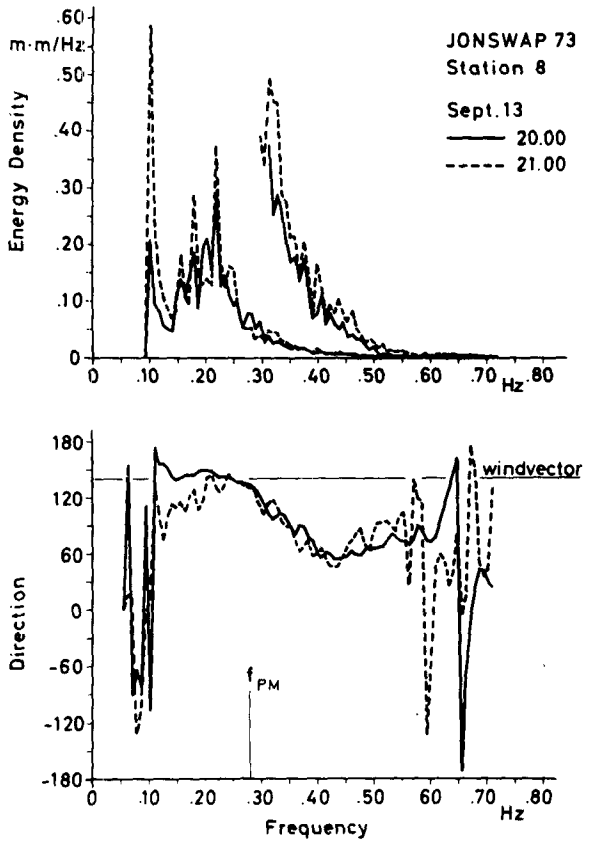

FIG. 5. (a) Power spectra for case c. The high-frequency region is shown 10 times enlarged. (b) The average wave direction spectra for case c. f_{PM} is defined in (7).

hourly wind sampling. This case shows, by the way, the difficulty to define directional parameters additional to θ_0 for resolving frequential distribution of the wind-sea.

From Fig. 4b we find the lowest frequency influenced by the new wind direction to be $f_m = 0.32$. From (26) this gives an effective angle $\theta = 32°$. The wind direction between 1900–2000 LT changes by about 100°, implying a change of $\theta_w - \theta_0$ from 0° to ~90°.

c. 13 September 1973 2000–2100 LT (MB) at station 8

The power and mean directional spectra of this case are given in figs. 5a and 5b. The wind vector direction is fairly constant and the mean wave angle changes by ~30°. The lowest frequency f_m which "feels" the wind direction is 0.43 Hz, which by (26) corresponds to $\theta = 49°$.

d. 21 September 1973 0815–1019 LT (PR) at station 10

This case, depicted in figs. 7a and 7b, shows slightly stronger wind than the previous ones. The second measurement shows the mean direction already aligned with the wind for frequencies larger than 0.36 Hz. If we take this as f_m in (26) we get an angle $\theta = -59°$.

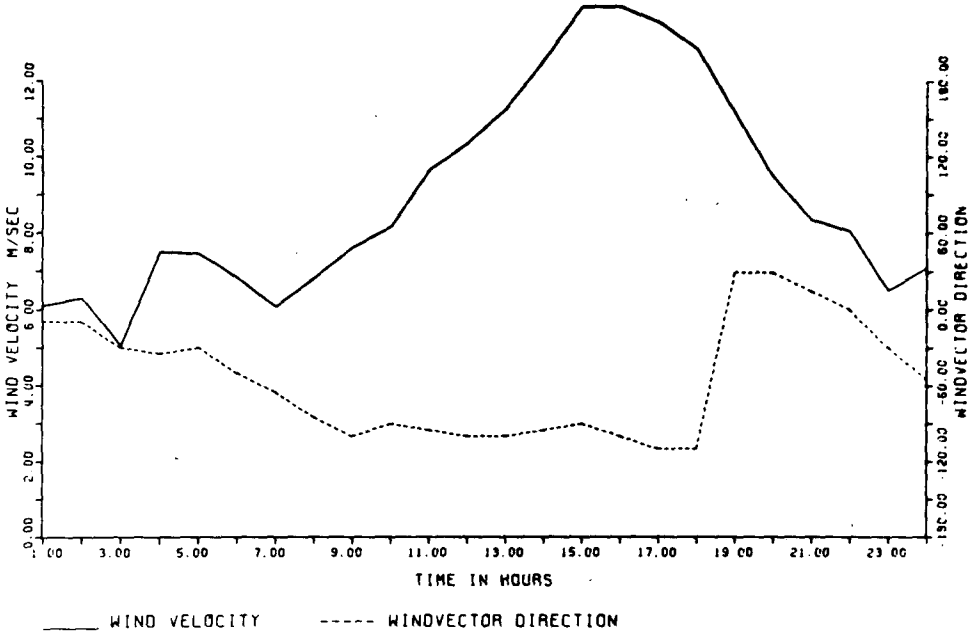

FIG. 6. Wind history on 21 September 1973 in the test area.

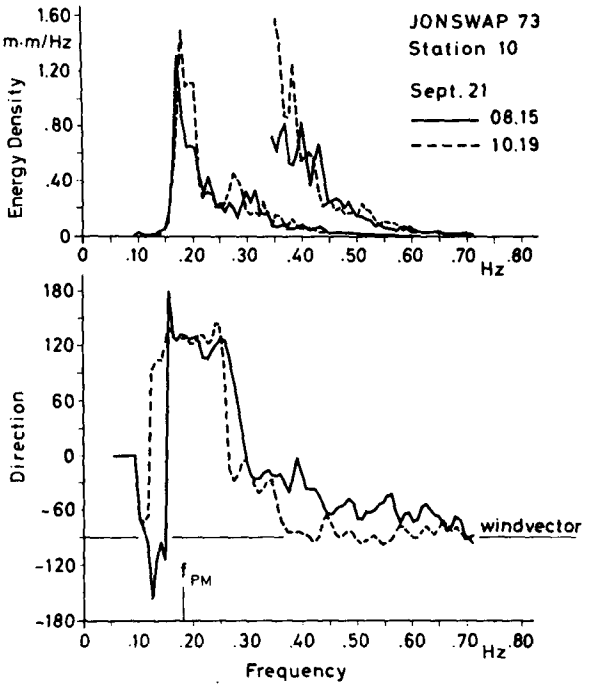

FIG. 7. (a) Power spectra for case d. The high-frequency region is shown 10 times enlarged. (b) The average wave direction spectra for case d. f_{PM} is defined in (7).

7. Summary

For a wind-sea spectrum of JONSWAP-type the prognostic equations were derived if the mean wave direction is added to the five JONSWAP parameters. The relaxation time for turning the mean wave direction into wind direction is defined for small angles to be

$$\tau = \left(\chi \frac{f_m^2}{g} U_{10}\right)^{-1},$$

where U_{10} is the wind velocity, g the gravitational constant and f_m the peak frequency, with $\chi = 0.21 \times 10^{-2}$ rad. We estimate the error involved in the determination of χ to be within $\pm 30\%$.

In the wave directional spectrum only frequency bands higher than the Pierson-Moskowitz frequency f_{PM} react to small shifts θ of wind direction relative to the average wave direction. For larger angular differences θ this frequency border f_b shifts to higher frequencies and the field data support

$$f_b = 0.13 \frac{g}{U''},$$

$$U'' = U_{10} \cos\theta, \quad |\theta| \leq \frac{\pi}{2},$$

where f_b, of course, becomes f_{PM} for vanishing θ.

Acknowledgments. This work was done within the "Sonderforschungsbereich 94", funded by the "Deutsche Forschungsgemeinschaft". We gratefully acknowledge the opportunity to use the data gathered by the participants of the JONSWAP-73 experiment.

APPENDIX

1. Functionals

The functional $\Phi_6(\mathbf{m})$ is defined in (13):

$$\theta_0 = \Phi_6[\mathbf{m}(f, \delta)] = \arctan M_x / M_y \qquad \text{(A1)}$$

with M_x, M_y defined in (11). The functional derivative calculated from (A1) is

$$\Phi_6'(\mathbf{G}(f, \delta)) = \frac{\int df \int d\delta (G_y \cos\theta_0 - \theta_x \sin\theta_0)}{\frac{8}{3\pi} \int df \frac{E(f)}{c(f)}}. \qquad \text{(A2)}$$

The other functionals Φ_i ($i = 1, \ldots, 5$) of (16) reproduce the JONSWAP parameters. The connected functional derivatives therefore are taken from previous publications (Günther *et al.*, 1979a).

2. Advection terms

The advection terms previously determined were

$$\tilde{D}_{ij} = \frac{8}{3\pi} \Phi_i'\left(|\mathbf{v}| \frac{\delta E}{\delta a_j}\right), \quad i, j = 1, \ldots, 5. \qquad \text{(A3)}$$

The D_{ijx}, D_{ijy} used in this paper easily can be shown to be

$$\left.\begin{aligned} D_{ijx} &= \tilde{D}_{ij} \sin\theta_0 \\ D_{ijy} &= \tilde{D}_{ij} \cos\theta_0 \end{aligned}\right\}. \qquad \text{(A4)}$$

The advection term coefficients $D_{i,6,x}$, $D_{i,6,y}$, $i = 1, \ldots, 5$ are evaluated by applying the functionals Φ_i', $i = 1, \ldots, 5$:

$$\left.\begin{aligned} \Phi_i'\left(v_x \frac{\delta \mathbf{m}}{\delta \theta_0}\right) &= D_{i6x} \\ \Phi_i'\left(v_y \frac{\delta \mathbf{m}}{\delta \theta_0}\right) &= D_{i6y} \end{aligned}\right\}. \qquad \text{(A5)}$$

It turns out that they are closely related to D_{i2}:

$$D_{i6x} = \begin{cases} -a_2 \tilde{D}_{i2} \cos\theta_0 \\ a_2 \tilde{D}_{i2} \sin\theta_0 \end{cases} \quad i = 1, \ldots, 5, \qquad \text{(A6)}$$

where D_{i2} is defined in (A3) and calculated in Günther *et al.* (1979a). a_2 is the Phillips-parameter α. For

$$\left.\begin{aligned} D_{6jx} &= \\ D_{6jy} &= \end{aligned}\right\} \Phi_6'\left(v_{x,y} \frac{\delta \mathbf{m}}{\delta a_j}\right) \quad j = 1, \ldots, 5, \qquad \text{(A7)}$$

the calculation gives

$$\begin{pmatrix} D_{6jx} \\ D_{6jy} \end{pmatrix} = \frac{3\pi}{8} \frac{g}{16\pi} \frac{\int df \frac{\delta E}{\delta a_j}}{\int dff E} \begin{pmatrix} -\cos\theta_0 \\ \sin\theta_0 \end{pmatrix}. \quad \text{(A8)}$$

In the same way

$$\begin{pmatrix} D_{66x} \\ D_{66y} \end{pmatrix} = \frac{3\pi}{8} \frac{g}{8\pi} \frac{\int df E}{\int dff E} \begin{pmatrix} \sin\theta_0 \\ \cos\theta_0 \end{pmatrix}. \quad \text{(A9)}$$

3. Source function

The treatment of the source function is again along the lines given in Günther *et al.* (1979a). In the treatment of the nonlinear part S_{nl} of the source function nothing changes. For the rest of the source function we assume a Snyder-Cox wind dependence defined in (18).

Now we apply our functionals Φ_i', $i = 1, \ldots, 5$, on the source function and arrive at the same expression as in the paper already cited, except that we get the wind component U'' along the mean wave direction θ_0 playing the part of $|\mathbf{U}|$:

$$S_2^{(in)} = 5.022 \times 10^{-3}(\nu'')^{4/3}\alpha f_m, \quad \text{(A10)}$$

where ν'' is defined in Section 5 [Eq. (21)]. Generalizing all arguments we arrive at the full source function:

$$S_1 = \begin{cases} -0.586 f_m^2 \left(\frac{\gamma - 1}{2.3}\right)\alpha^2, & \gamma > 1 \\ 0, & \text{otherwise} \end{cases}$$

$$S_2 = (5.022 \times 10^{-3}(\nu'')^{4/3} - 5\alpha^2)\alpha f_m$$

$$S_3 = -16.0(\gamma - \gamma_0)\alpha^2 f_m$$

$$S_4 = -[25.5(\sigma_a - 0.07h) - 0.5(\sigma_b - 0.09h)]\alpha^2 f_m$$

$$S_5 = -[25.5(\sigma_b - 0.09h) - 0.5(\sigma_a - 0.07h)]\alpha^2 f_m$$

$$\gamma_0 = \begin{cases} 3.3, & \nu'' \geq 0.16 \\ 1 + 2.3\frac{\nu'' - 0.13}{0.03}, & 0.16 \geq \nu'' \geq 0.13 \\ 1, & 0.13 \geq \nu'' \end{cases}$$

$$h = \left(\frac{4.0}{\gamma + 0.7}\right)^2. \quad \text{(A11)}$$

For S_6 we obtain

$$S_6 = S_6^{in} = -\chi U_\perp \frac{f_m^2}{g}, \quad \text{(A12)}$$

where $U_\perp$ is the wind vector component normal to the mean wave direction.

REFERENCES

Cardone, V. J., D. B. Ross and M. R. Ahrens, 1977: An experiment in forecasting hurricane generated sea states. *Preprints 11th Tech. Conf. Hurricanes and Tropical Meterology*, Miami, Amer. Meteor. Soc., 688–695.

Ewing, J. A., 1980: Observations of wind-waves and swell at an exposed coastal location. *Estuarine Coastal Mar. Sci.*, **10**, 543–554.

Garrett, C., and J. Smith, 1976: On the interaction between long and short surface waves. *J. Phys. Oceanogr.*, **6**, 925–930.

Günther, H., W. Rosenthal and K. Richter, 1979b: Application of the parametrical surface wave prediction model to rapidly varying wind fields during JONSWAP 1973. *J. Geophys. Res.*, **84**, 4855–4864.

——, ——, T. J. Weare, B. A. Worthington, K. Hasselmann and J. A. Ewing, 1979a: A hybrid parametrical wave prediction model. *J. Geophys. Res.*, **84**, 5727–5738.

Hasselmann, D. E., M. Dunckel and J. A. Ewing, 1980: Directional wave spectra observed during JONSWAP 1973. *J. Phys. Oceanogr.*, **10**, 1264–1280.

Hasselmann, K., 1974: On the spectral dissipation of ocean waves due to white capping. *Bound. Layer Meteor.*, **6**, 107–127.

——, D. B. Ross, P. Müller and W. Sell, 1976: A parametric wave prediction model. *J. Phys. Oceanogr.*, **6**, 200–228.

——, T. P. Barnett, E. Bouws, H. Carlson, D. E. Cartwright, K. Enke, J. A. Ewing, H. Gienapp, D. E. Hasselmann, P. Kruseman, A. Meerburg, P. Müller, D. J. Olbers, K. Richter, W. Sell and H. Walden, 1973: Measurements of wind, wave-growth and swell decay during the Joint North Sea Wave Project (JONSWAP). *Ergänz. Dtsch. Hydrogr. Z.*, Suppl. A., **8**, No. 12, 95 pp.

Kawai, S., P. S. Joseph and Y. Toba, 1979: Prediction of ocean waves based on the single-parameter growth equation of wind waves. *J. Oceanogr. Soc. Japan*, **35**, 151–167.

King, D. B., and O. H. Shemdin, 1978: Remote sensing of hurricane waves. *Proc. Int. Conf. Coastal Engineering*, Hamburg.

Miles, J. W., 1957: On the generation of surface waves by shear flows. *J. Fluid Mech.*, **3**, 185–204.

——, 1959: On the generation of surface waves by shear flows. Part 2. *J. Fluid Mech.*, **6**, 568–582.

Müller, P., 1976: Parametrization of one-dimensional wind-wave spectra and their dependence on the state of development. *Hamburger Geophys. Einzelschriften*, **31**, University of Hamburg.

Phillips, O. M., 1977: *The Dynamics of the Upper Ocean*, 2nd ed. Cambridge University Press, 291 pp.

Resio, D. T., and C. L. Vincent, 1979: A comparison of various numerical wave prediction techniques. *Proc. 11th Offshore Technology Conference*, Houston, 2471–2478.

Snyder, R. L., and C. S. Cox, 1966: A field study of the wind generation of ocean waves. *J. Mar. Res.*, **24**, 141–178.

——, F. W. Dobson, J. A. Elliot and R. B. Long, 1980: Array measurements of atmospheric pressure fluctuations above surface gravity waves. Submitted to *J. Fluid Mech.*

Toba, Y., 1978: Stochastic form of the growth of wind waves in a single-parameter representation with physical implications. *J. Phys. Oceanogr.*, **8**, 494–507.